

## Subwavelength dynamic focusing in plasmonic nanostructures using time reversal

Guy Bartal,<sup>1</sup> Geoffroy Lerosey,<sup>1,\*</sup> and Xiang Zhang<sup>1,2,†</sup>

<sup>1</sup>NSF Nanoscale Science and Engineering Center (NSEC), 5130 Etcheverry Hall, University of California, Berkeley, California 94720-1740, USA

<sup>2</sup>Materials Sciences Division, Lawrence Berkeley National Laboratory, 1 Cyclotron Road, Berkeley, California 94720, USA  
(Received 20 March 2008; published 7 May 2009)

We employ time reversal for deep subwavelength focusing in plasmonic periodic nanostructures. The strong anisotropy enables propagating modes with very large transverse wave vector and moderate propagation constant, facilitating transformation of diffraction-limited plane waves to high- $K$  Bloch waves in the plasmonic nanostructure. Time reversal is used to excite the waves in the nanostructure at the exact amplitude and phase to focus the incident light to dimensions well below the diffraction limit at any point in the structure, exemplifying a true subdiffractional confinement and resolution.

DOI: 10.1103/PhysRevB.79.201103

PACS number(s): 42.25.Bs, 73.20.Mf

Focusing light to dimensions smaller than its wavelength has gained increasing attention, both for its potential applications in lithography, spectroscopy, and telecommunication; and the intriguing challenge of beating the diffraction limit. Sub- $\lambda$  focusing of light was first achieved using very sharp tips or nanoparticles,<sup>1-3</sup> acting as “pointlike” scatterers which convert propagating waves to evanescent ones, with a relatively low efficiency. Nanofocusing (NF) techniques, relying on increasing the wave number during propagation in a plasmonic waveguide of varying widths,<sup>4,5</sup> offer a more efficient conversion. While these schemes can provide good confinement, they are rather complicated to fabricate, and limited to a fixed focus point.

To date, deep sub- $\lambda$  focusing has not been achieved in systems with translational symmetry (e.g., homogeneous media or photonic crystals), as these are known not to support the high  $k$  vectors required for the strong light confinement. Such systems, however, can have flexible focus position, as there is no predetermined structural focal point. Combining the tunable capabilities of these systems with the strong confinement found in plasmonic structures, one could obtain a powerful tool, applicable to numerous applications in lithography, sensing and telecommunications. This combination is found in plasmonic structures, for example, a metal-dielectric multilayer (MDML) composite with nanoscale period. These anisotropic translation invariant systems can support propagating modes with very large transverse wave vector but with moderate wave numbers. Though being simple and easy to fabricate, MDMLs are rich in their characteristics and provide both intriguing physical behavior and various applications.<sup>6-8</sup> Recently, such a multilayer system was proposed as a plasmonic lens,<sup>9</sup> but owing to the lack of coupling to the modes with large transverse wave vector, the smallest focal spot obtained was limited by the index of the surrounding medium (namely,  $\lambda/2n_{\text{dielectric}}$ ).

Here, we present dynamic deep subwavelength focusing in plasmonic nanostructures. These structures support propagating modes with very high transverse wave vector, enabling the deep subwavelength confinement. At the same time, the moderate values of the wave numbers (“propagation constants”) associated with these modes allow for transformation of plane waves (that are diffraction limited in the surrounding area) to the high- $K$  modes of the plasmonic structures. Using time reversal (TR), we can excite these

modes with the proper amplitude and phase to control their interference so as to create a highly localized focal spot (down to 30 nm at 1.55  $\mu\text{m}$  wavelength) at any desired position in the structure.

Focusing in homogeneous media occurs when a sum of plane waves is coherently added to interfere constructively within a small spot and destructively over the rest of the space. The smallest spot size that can be obtained depends on the transverse wave vector of the plane waves, which is limited by the wavelength,  $\lambda$ , and the refractive index of the medium,  $n$ .

This restriction arises from the relation between the transverse wave vector and the wave number  $k_x^2 + k_z^2 = n^2 (\frac{2\pi}{\lambda})^2$  where  $k_x$  represents the transverse wave vector and  $k_z$  is the wave number (propagation constant). As any  $k_x$  larger than  $(\frac{2\pi n}{\lambda})$  results in an imaginary propagation constant  $k_z$  (i.e., a nonpropagating field), a beam cannot be focused to dimensions smaller than the order of the wavelength in the medium.

Conversely, metal-dielectric composites give rise to surface plasmon-polaritons (SPP). These are bound surface waves that decay exponentially normal to the surface<sup>10</sup> and, hence, remain confined to dimensions much smaller than the wavelength. Namely, these waves propagate along the metal-dielectric interface with *imaginary*,  $k_x$  enabling *real* propagation constant  $k_z$  larger than  $(\frac{2\pi n}{\lambda})$ . MDMLs, comprised of nanometer-scale alternating layers of metal and dielectric slabs, allow SPP tunneling, forming “plasmonic Bloch modes” (Fig. 1).<sup>11</sup> At frequencies far from the plasmon resonance,<sup>10</sup> the MDML can be designed such that the penetration depth in the dielectric is much larger than that in the metal,<sup>8</sup> in contrast to most layered metal-dielectric metamaterials applications.<sup>7,12,13</sup> In this regime, the structure can be considered as an array of dielectric waveguides evanescently coupled through the metal slabs, where the wave propagation is along the metal-dielectric interface (as opposed to Refs. 7, 12, and 13 where the propagation is normal to the interfaces). Interestingly, the evanescent nature of the electric and magnetic field in the direction normal to the surfaces allows to shrink the metal and dielectric slabs to dimensions much smaller than the wavelength, while still maintaining mode propagation along the surfaces. Furthermore, since the system is in the regime far from plasmon resonance, such modes

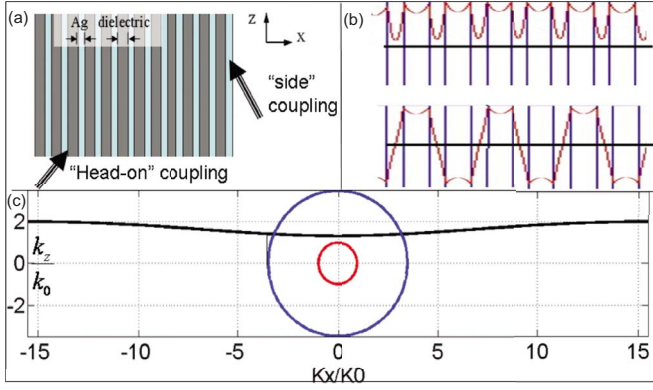


FIG. 1. (Color online) (a) Schematics of the MDML, exemplifying “Head on coupling” and “side coupling” approaches. (b) Photonic SPP Bloch modes (magnetic field,  $H_y$ ) associated with the MDML. Top:  $Kx=0$ . Bottom:  $Kx=\pi/D$ . (c) “Diffraction relations” of 20 nm Ag and 30 nm air MDML at 1.55  $\mu\text{m}$  wavelength (Black line), compared with the equivalent relations in vacuum (red/gray circle) and semiconductor with  $n=3.5$  (blue/dark gray circle). The axes are normalized with the vacuum wave vector  $k_0$ .

can have long propagation length compared to the near-resonance structures. This results in large (and real) Bloch  $K$  vectors (up to  $\pi/D$ , with  $D$  being the structure period) associated with moderate propagation constants  $k_z$  (about two times the wave number in vacuum). Coherent interference of these modes can produce a highly confined spot which is limited only by the period size of the MDML.

The array under consideration is composed of alternating thin films of air (30) and silver (20 nm), with the metal permittivity at  $\lambda=1.55 \mu\text{m}$  being  $\epsilon_m=-130+3.7i$ .<sup>14</sup> The diffraction relation of this system, showing the relations between  $k_z$  and  $k_x$ , is presented in Fig. 1(c) along with the circularly symmetric diffraction relations of vacuum and silicon (with  $n=3.5$ ). The relations are normalized to the wave vector in vacuum  $k_0=(\frac{2\pi m}{\lambda})$  and obtained by solving directly Maxwell’s equation.<sup>8</sup> Clearly, the MDML features a highly anisotropic response, with the transverse wave vector extending up to  $k_x \approx 15k_0$ .

The main challenge in such media is to couple efficiently light from the diffraction-limited  $k$  vectors in a homogeneous medium (e.g., air or dielectric with  $n \leq 3.5$ ) to the high  $k$  vectors of the MDML (with  $k_x \approx 15k_0$ ). Coupling light to the waveguides by “head on” coupling [see Fig. 1(a)] results in direct excitation of the transverse Bloch  $k$  vectors,  $k_x$ . As the wave vectors outside the MDML are limited by the refractive index in the surrounding medium, the largest  $k_x$  that can be phase matched in the MDML cannot be larger than that outside. Even when carving the MDML with a lens shape,<sup>9</sup> the conservation of the momentum at the interface imposes an upper limit to the excited  $k_x$ , and the focal spot is once again diffraction limited. On the other hand, coupling light from the structure sides [“side coupling,” also presented in Fig. 1(a)] gives rise to excitation of the Bloch modes by phase matching to the propagation constant,  $k_z$ , that is conveniently moderate in magnitude. This scheme is simulated in Fig. 2, where a Bloch mode with a propagation constant  $k_z=1.9k_0$  is excited via “side coupling” from a surrounding dielectric

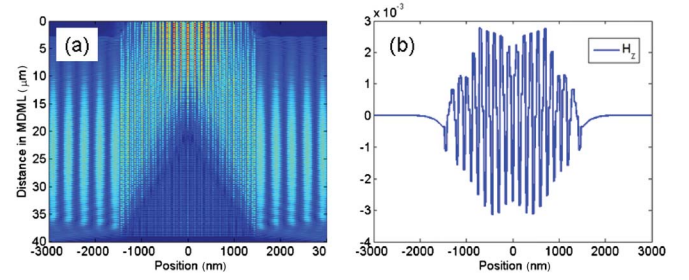


FIG. 2. (Color online) (a) The modulus of the magnetic field inside the waveguide array and in the host dielectric, exemplifying the excitation of a Bloch mode. (b) The profile of the magnetic field at the output of the waveguide array is shown in Fig. 2

medium (refractive index of 2.2, e.g., ZnS), by a 20- $\mu\text{m}$ -wide Gaussian beam. The exciting plane wave is tilted in an angle  $\theta$  such that its longitudinal wave vector  $k_z=n \cdot k_0 \cdot \cos \theta$  is equal to the propagation constant of the Bloch mode with  $k_z=1.9k_0$ . Evidently, the phase matching condition between the plane wave in the high-index dielectric and the plasmonic Bloch wave in the MDML resides in an efficient excitation of a mode with a spatial period of about 150 nm, which corresponds to  $k_x \approx 5k_0$ —well below the diffraction limit in the surrounding medium. As all of the modes’ effective indices (propagation constants divided by the wave vector in vacuum,  $n_{\text{eff}}=k_z/k_0$ ) are smaller than the surrounding medium refractive index [see Fig. 1(c)], the Bloch modes in this system can all be excited by simply varying the angle of incidence of the Gaussian beam.

To understand the role of TR in the focusing mechanism, we start by analyzing the wave propagation inside the periodic metal-dielectric nanostructure: a highly confined wave packet at the structure input can be considered as a coherent interference of the system’s eigenmodes, noted by  $\psi_n$ . Namely, the field can be expressed as  $\phi(x)=\sum_n a_n \psi_n(x)$  where  $a_n$  indicates the wave-packet projection on the mode  $\psi_n$ , which can be either the electric field, magnetic field or a vector comprises both fields (see, e.g., Ref. 8). In vacuum, for example, the modes of the system are plane waves tilted at different angles and represented by  $k_x=k_0 \cdot \sin \theta$ . The eigenvalues are  $k_z=\sqrt{k_0^2-k_x^2}=k_0 \cdot \cos \theta$ . Likewise, in periodic structures the modes will carry the characteristic system periodicity, where in MDML the wave propagation is at a form of plasmonic Bloch modes.<sup>8,11</sup>

As each mode acquires different phase when propagating in the waveguide array [depending on  $k_z$ , see Fig. 1(c) for vacuum, silicon and MDML], the constituent modes of the wave packet are no longer in phase and the wave packet diffracts as it propagates. Its evolution after a propagation distance  $d$  is given by  $\phi(x,d)=\sum_n a_n \psi_n(x) e^{-i\beta_n d}$ , where  $\beta_n$  are the eigenvalues and represent the propagation constants of the  $n$ th mode of the system (replacing the notation  $k_z$ ). The question arising is whether it is possible to obtain this mechanism in a reversed chronology so as to focus electromagnetic waves on a deep sub- $\lambda$  scale.<sup>15</sup>

The answer lies in the principle of TR.<sup>16</sup> In a typical TR experiment, a source emits a wave field which propagates inside a medium and is recorded on a closed surface. The signal is then flipped in time (similar to phase conjugation at

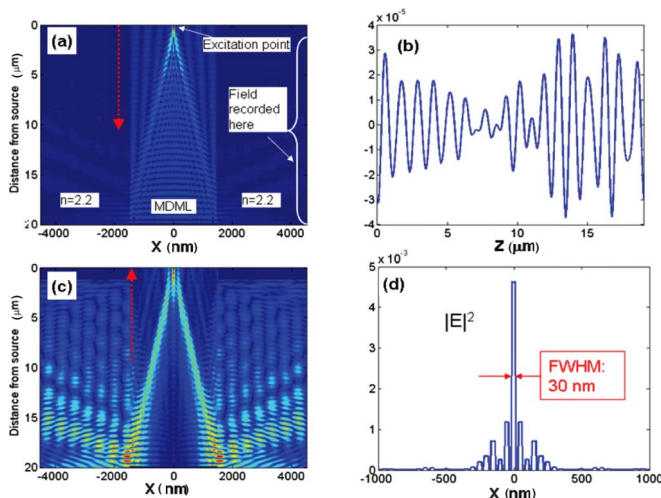


FIG. 3. (Color online) Using time reversal for subwavelength focusing. The red arrows indicate the propagation direction. (a) The modulus of the magnetic field for excitation of a single waveguide in the array (MDML). The “source” is at the top center of the array and the emerging field is recorded in the dielectric medium. (b) The amplitude of the recorded magnetic field. (c) The modulus of the magnetic field for excitation of the array with the time-reversed field. (d) The electric-field intensity at the array output after TR.

each frequency), and sent back into the medium. It has been shown that the waves created by the TR propagate backward in the medium and focus at the same location as the original source.<sup>17–19</sup> Very recently, it has also been shown in microwave frequencies that by placing the original source in a disordered microstructured media, TR focusing can overcome the diffraction limit.<sup>20</sup> Here, we apply TR in the spatial domain, i.e., we “reverse” the diffraction of a highly confined beam at a single frequency, and focus near IR waves down to a spot whose size is limited only by the waveguide array.

Interestingly, using TR together with “side coupling” between a high-index dielectric medium and the MDML, one can focus the incident wave at any point in the array, simply by controlling the fields at the interfaces between the MDML and the host dielectric, evading the need to control the field on a sub- $\lambda$  scale inside the plasmonic structure. For convenience, we choose the focal point to be at the array output face.

The principle of spatial TR for sub- $\lambda$  focusing is demonstrated in Fig. 3 for the structure considered in Fig. 1. The silver and air layer thickness are 20 and 30 nm, respectively. The dielectric host has a refractive index of 2.2 (e.g., ZnS) and its width is 2  $\mu\text{m}$  on each side, corresponding to twice the wavelength. This is to ensure that no evanescent wave information is recorded.

As a first step, we excite a single waveguide of the MDML from the output face [top of Fig. 3(a)]. The light tunnels between the waveguides as it propagates until it is coupled out to the surrounding dielectric [Fig. 3(a)]. The emerging field (which is diffraction limited) is recorded at the boundaries of the host dielectric [see Fig. 3(b)] and “time reversed” (i.e., phase conjugated<sup>21</sup>). Note that the spatial period of the recorded field is of the order of 1.1  $\mu\text{m}$ , which is

consistent with the fact that only diffraction-limited waves are recorded (no evanescent contribution). Experimentally, the recorded pattern can then be applied to a spatial light modulator (SLM) to transform an incident plane wave to the sum of spatial frequencies (plane waves with the proper phase relations) that create the “time-reversed” field. These waves are coupled back to the periodic structure, exciting the high spatial frequency modes that propagate “backwards” in the array and interfere constructively to form a localized beam at the exact location of the initial emitting source [Fig. 3(c)], which was chosen to be at the array output.

We underline a clear analogy between time reversal in the temporal domain,<sup>16–19</sup> and our approach which lies in the spatial domain. While TR experiments have shown compensation for temporal dispersion, our approach compensates for spatial dispersion. This is to say, while in the time domain each frequency component propagates backward at its own phase velocity, compensating for the phase lag accumulated in the emitting step, the same mechanism occurs here for the spatial frequencies, propagating back with a propagation constant of the same magnitude (and opposite sign).

The time-reversed beam intensity at the MDML output is plotted in [Fig. 3(d)]. The intensity full width at half maximum (FWHM) is limited by the width of the dielectric waveguide, to 30 nm. Namely, the diffraction-limited waves in the host dielectric (with  $n=2.2$ ), were transformed to high- $K$  waves in the metal-air nanostructure, realizing focusing of near-IR radiation on a spot whose width is of the order of  $\lambda/50$ ,  $\lambda$  being the wavelength in free space.

Note that the focal spot created by TR [Figs. 3(c) and 3(d)] differ from the original sources in Fig. 3(a). Namely, weaker secondary spots (side lobes) are observed aside of the focal spot. These are the result of the mode loss in the MDML; as the high-(spatial) frequency modes suffer higher loss, they dissipate during propagation more than their low-frequency counterparts, resulting in imperfect TR. To counteract this effect, one can use inverse filtering (IF).<sup>22</sup> Namely, correcting the weight of each spatial frequency of the signal recorded on the dielectric boundaries. This will result in a perfect focal spot without side lobes.

The focusing efficiency (the ratio between the power in the focal spot and the power input on the boundaries of the dielectric host) can be estimated by dividing the power contained in the focal spot by the total power of the incident (diffraction limited) wave. We estimate the efficiency to be around 15%, which is comparable to that of bulk wave conversion to SPP in metal-coated tapered optical fiber.<sup>23</sup> Naturally, as the use of IF involves distributing more energy in modes with higher loss, it increases the total propagation loss, hence affecting the focusing efficiency.

Contrary to nanofocusing configurations which allow focusing to a single predetermined point, flexibility in the focal position of plasmonic devices will be useful for various applications.<sup>24</sup> Our method enables flexibility in the positioning of the deep subwavelength focal spot. Similar to the focal spot obtained at the center of the array in Fig. 3, the TR operation can be used to focus beam on any position in the array, simply by repeating the TR procedure for different excitation positions. Each desired focus position will result in a different corresponding diffraction-limited field pattern

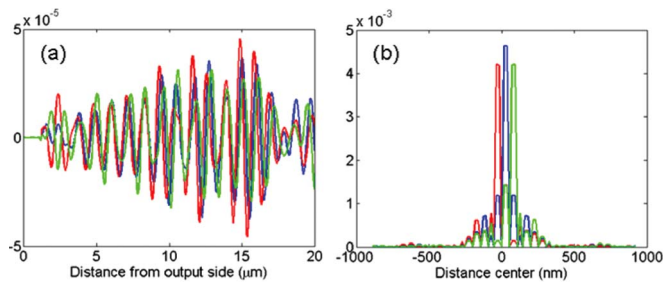


FIG. 4. (Color online) (a) The fields recorded in the dielectric medium, for three different excitations of adjacent waveguides. (b) The corresponding focal spots obtained by time reversal at the array output

in the host dielectric. A focal spot “library” can then be recorded and used in order to dynamically control the position of the focal spot in the waveguide array, allowing one to “turn on” any waveguide in a MDML, while the achievable resolution is only limited by the period of the array. This concept is illustrated in Fig. 4, where we show the recorded fields on the boundary of the dielectric medium, for three different adjacent sources [Fig. 4(a)], as well as the corresponding focal spots obtained by time reversal [Fig. 4(b)]. Although two adjacent foci are separated by only 1 period of the array (i.e., 50 nm), the recorded corresponding fields can be clearly resolved, and contain the spatial information of each focal point, allowing focusing at a resolution of 50 nm, on 30-nm-wide focal spots. Since the system is lossy, focusing on noncentered waveguides results in asymmetric and hence broader focal spots [see Fig. 4(b)]. This can be corrected using IF or by modifying the pattern on each side of the MDML.

Finally, we address the possible experimental implementation of this concept. While thin-film fabrication is already well established, and the structure itself can be fabricated using routine nanofabrication with low-index dielectric, temporal time reversal has never been demonstrated in optical

frequencies as it is impossible to measure and control the phase and amplitude of optical waves. In the spatial domain, however, SLMs allow one to control the amplitude and phase of an optical wave over thousands of pixels, and in fact, have already been used to focus light through an opaque scattering media, utilizing spatial TR for diffraction-limited focusing through minimization algorithms.<sup>25</sup> The patterns to be recorded and used on the SLM can be obtained by exciting any waveguide in the array with a sharp tip, or simply by numerical simulation of such an excitation. The SLM can then be used to modulate an incident plane wave, resulting in focusing at the desired point. Such approach would allow the tunability of the focal spot position with a speed limited by the switching time of the SLMs, which can be lower than a millisecond. This concept can be further expanded to two-dimensional (2D) system, using e.g., sub- $\lambda$  nanohole arrays.<sup>26</sup> In fact, the concept of efficient conversion of high-spatial frequency modes to diffraction-limited waves and back can be utilized as an efficient “far-field superlens,”<sup>27</sup> which will be able to record and image over long distances 2D objects with deep sub- $\lambda$  features.

To conclude, we have demonstrated a method based on the high anisotropy of metal-dielectric multilayers that allows one to couple efficiently bulk (low-spatial frequency) plane waves to the high-spatial frequency modes of such structures. Using time-reversal methods, we showed numerically that we are able to focus near IR waves down to a spot limited by the period of the structure, which can be much smaller than the wavelength in the surrounding medium. We obtained focal spots as small as  $\frac{1}{50}$  of a wavelength, and were able to control their position with a 50 nm resolution. We believe that this concept can prove useful in many applications.

This work is supported by DARPA (Agreement No. HR0011-05-3-0002), the U.S. Army Research Office (ARO) MURI program 50432-PH-MUR, and the NSF under Grant No. CMMI-0751621. The authors thank Rupert Oulton and David Pile for stimulating discussions.

\*Present address: Laboratoire Ondes et Acoustique, École Supérieure de Physique et de Chimie Industrielles, Université Paris VII, Centre National de la Recherche Scientifique, UMR 7587, 10 rue Vauquelin, 75005 Paris, France.

†Corresponding author: xzhang@me.berkeley.edu

<sup>1</sup>L. Novotny *et al.*, *Ultramicroscopy* **61**, 1 (1995).

<sup>2</sup>Shuming Nie and Steven R. Emory, *Science* **275**, 1102 (1997).

<sup>3</sup>S. A. Maier, *et al.*, *Appl. Phys. Lett.* **81**, 1714 (2002).

<sup>4</sup>M. I. Stockman, *Phys. Rev. Lett.* **93**, 137404 (2004).

<sup>5</sup>D. F. P. Pile and D. K. Gramotnev, *Appl. Phys. Lett.* **89**, 041111 (2006); H. Choi *et al.*, *Optics Express* **17**, 7519 (2009).

<sup>6</sup>M. Scalora *et al.*, *J. Appl. Phys.* **83**, 2377 (1998).

<sup>7</sup>P. A. Belov and Y. Hao, *Phys. Rev. B* **73**, 113110 (2006).

<sup>8</sup>Y. Liu *et al.*, *Phys. Rev. Lett.* **99**, 153901 (2007).

<sup>9</sup>X. Fan and G. P. Wang, *Opt. Lett.* **31**, 1322 (2006).

<sup>10</sup>H. Raether, *Surface Plasmons: On Smooth and Rough Surfaces and on Gratings* (Springer, Berlin, 1988).

<sup>11</sup>J. Schilling, *Phys. Rev. E* **74**, 046618 (2006).

<sup>12</sup>Z. Liu *et al.*, *Science*, **315**, 1686 (2007); H. S. Lee *et al.*, *New J.*

*Phys.*, **7**, 255 (2005); X. Zhang and Z. Liu, *Nature Mater.* **7**, 435 (2008).

<sup>13</sup>A. J. Hoffman *et al.*, *Nature Mater.* **6**, 946 (2007).

<sup>14</sup>P. B. Johnson and R. W. Christy, *Phys. Rev. B* **6**, 4370 (1972).

<sup>15</sup>P. St. J. Russell, *Appl. Phys. B* **39**, 231 (1986); D. Mandelik *et al.*, *Phys. Rev. Lett.* **90**, 053902 (2003).

<sup>16</sup>M. Fink, *Phys. Today* **50**(3), 34 (1997).

<sup>17</sup>G. Lerosey *et al.*, *Phys. Rev. Lett.* **92**, 193904 (2004).

<sup>18</sup>G. Lerosey *et al.*, *Appl. Phys. Lett.* **88**, 154101 (2006).

<sup>19</sup>R. Carminati *et al.*, *Opt. Lett.* **32**, 3107 (2007).

<sup>20</sup>G. Lerosey *et al.*, *Science* **315**, 1120 (2007).

<sup>21</sup>R. W. Hellwarth, *J. Opt. Soc. Am.* **67**, 1 (1977).

<sup>22</sup>M. Tanter *et al.*, *J. Acoust. Soc. Am.* **110**, 37 (2001).

<sup>23</sup>W. Ding *et al.*, *Phys. Rev. A* **75**, 063822 (2007).

<sup>24</sup>Z. Liu *et al.*, *Appl. Phys. Lett.* **88**, 171108 (2006).

<sup>25</sup>I. M. Vellekoop and A. P. Mosk, *Opt. Lett.* **32**, 2309 (2007).

<sup>26</sup>H. Masuda and K. Fukuda, *Science* **268**, 1466 (1995).

<sup>27</sup>Z. Liu *et al.*, *Nano Lett.* **7**, 403 (2007).